ORIGINAL PAPER

Development of nano IrO$_2$ composite-reinforced nickel–phosphorous electrodes for hydrogen evolution reaction

S. M. A. Shibli · V. S. Dilimon

Abstract Electroless and electroplated nickel electrodes are extensively used for hydrogen evolution reaction (HER). In the present work, TiO$_2$-supported IrO$_2$ mixed oxide composite was prepared and used to reinforce Ni–P electroless plates to be used as catalytic electrodes for HER. The electrodes exhibited high electrocatalytic activity when the electrodes were used for HER. All the parameters including particle size of the catalyst, surface roughness, and surface active sites were studied. The particle size of the IrO$_2$ catalyst in the mixed oxide was found to have high influence on the catalytic activity of the electrodes. Low overpotential as low as 70 mV at a current density of 200 mA cm^{-2} was achieved with the mixed oxide-reinforced Ni–P electrodes.

Keywords Hydrogen evolution · Electrocatalysis · Electroless nickel coating · Iridium dioxide catalyst · Composite reinforcement · Catalytic electrode

Introduction

One of the major problems of today's world is the crisis in fossil fuels on which the world depends heavily. The availability of fossil fuels will decrease in the coming years while the utilization of fossil fuels is predicted to decrease exponentially [1]. Hence, alternative sustainable energy resources are desired. Hydrogen, an alternative ideal fuel, can be considered as the fuel of the future, as it is abundant and has many advantages like being environmental friendly.

The production of hydrogen by electrolysis of water has major setbacks such as high-energy consumption, low specific production rates, and low efficiency. A possible remedy for these problems is the use of electrocatalytic electrodes for the water electrolysis. Industrial water electrolysis is generally carried out using electrocatalytic electrodes as cathodes and liquid alkaline water as electrolyte. Oxides of cobalt [2], ruthenium [3–5], iridium [6–8], and titanium are used as electrocatalysts for hydrogen evolution reaction (HER) in alkaline and acidic solutions. Electrolytic Ni–P plates having RuO$_2$ [3–5, 10, 11] and electroless Ni–P plates having ZrO$_2$ are also reported to be highly active for HER [12].

Electroless and electroplated Ni–P electrodes are extensively used for HER [13, 14]. In our previous study, we have developed ZrO$_2$-reinforced catalytic Ni–P electroless plates for HER [12]. IrO$_2$ has been known to be an effective catalyst for HER [6–8]. TiO$_2$ is a good catalytic support of RuO$_2$ and IrO$_2$ electrocatalysts. It is also a good composite for reinforcing Ni–P plates resulting in improvement of physico-chemical properties of the plates. In the present work, TiO$_2$-supported IrO$_2$ mixed oxide composite was prepared and used to reinforce Ni–P electroless plates to be used as catalytic electrodes for HER.

Experimental methods

Preparation and characterization of the TiO$_2$-supported IrO$_2$ mixed oxide

Two different methods were adopted for the preparation of TiO$_2$-supported IrO$_2$ mixed oxide. In the first method, the

S. M. A. Shibli (✉) · V. S. Dilimon
Department of Chemistry, University of Kerala,
Kariavattom Campus,
Trivandrum, Kerala 695 581, India
e-mail: smashibli@yahoo.com

required amount of IrCl$_3$ was dissolved in isopropanol. TiO$_2$ powder of particle size ~30 nm (Merck, India) was socked in the isopropanol solution of IrCl$_3$ for 30 min with continuous stirring. The solvent was slowly evaporated in a beaker until a dry mixture was obtained. The mixture was then heated at 250 °C for 1 h in an oven. The mixtures were finely powdered and heated for one more hour. The powder was then fired at 450 °C in a muffle furnace for 1 h for complete conversion of IrCl$_3$ into IrO$_2$. This method of TiO$_2$-supported IrO$_2$ mixed oxide preparation is named as thermal decomposition (TD) method in this paper.

In the second method, nano size IrO$_2$ particles were prepared by Adams fusion technique [15]. To synthesize the IrO$_2$, an iridium chloride precursor (Merck) was oxidized within a sodium nitrate (Merck) melt. To disperse the precursor evenly throughout the excess of NaNO$_3$, the salts were dissolved in isopropanol and the solvent slowly evaporated until a dry salt mixture was obtained. Typically, 10 g of NaNO$_3$ and 0.2 g precursor were prepared in a 100-ml beaker. The dry salt mixture was then placed into a preheated furnace. The temperature of this melt was maintained at 500 °C for 30 min. The oxidized iridium particles were separated from the fused salt mixture by dissolving the remaining salts in water and by centrifugation after adding TiO$_2$ powder (Merck), having particle size of ~30 nm, into the solution with vigorous stirring. The mixed oxide powder was then dried at 200 °C for 3 h. The X-ray diffraction (XRD) analysis of the mixed oxide confirmed the complete conversion of IrCl$_3$ to IrO$_2$. This method of TiO$_2$-supported IrO$_2$ mixed oxide preparation is named as thermal oxidation (TO) method in this paper. The particle size of the mixed oxide was analyzed by using transmission electron microscopy.

Electroless plating

Mild steel coupons having composition of 0.09% carbon, 0.034% manganese, 0.036% phosphorus, 0.0487% silicon, and 0.029% aluminum were used as the substrate for plating. The dimension of the mild steel substrates was 5×6×0.4 cm. The substrates were cleaned mechanically and then washed with distilled water. The substrates were treated in 5% NaOH and then in 3% HCl for 5 min. The treated substrates were then sensitized in a solution containing 10 g/l SnCl$_2$ in 40 ml/l HCl (37%). After sensitization, the surface was activated in a solution of 1g/l PdCl$_2$ in 10 ml/l HCl (37%).

Electroless plating was carried out at 90 °C in a 500 ml glass vessel with continuous stirring. To reduce the loss of bath components and to maintain the pH, the glass vessel was closed with a lid having two openings, one for the insertion of coupon and the other for the insertion of a sensitive thermometer. The composition of the electroless

bath was: 30 g/l nickel sulfate, 25 g/l succinic acid, and sodium 25 g/l hypophosphite. The initial pH of the bath was 1.9–2.0 due to the presence of succinic acid. The bath pH was adjusted to 4.5 by adding ammonia solution. It has been reported that the concentration of 10 g/l TiO$_2$ in the electroless nickel bath is the optimum for the preparation of better quality Ni–P plate reinforced with TiO$_2$ [16]. In the present work also, during the preliminary study, 10 g/l mixed oxide was found to develop better quality plate. Hence, 10 g/l mixed oxide was added into the bath during preparation of the composite plates. The mixed oxide powder of required quantity was added into the bath with constant stirring, soon after making the bath ready for plating and before the initiation of the plating process. The plating process was continued with constant stirring of the bath at a pre-optimized speed. The temperature and pH of the bath were maintained. The plated specimens were taken out, rinsed with distilled water, and kept ready for evaluation.

Physico-chemical characterization

Physical characteristics of the plates such as hardness, thickness, adherence, and wear resistance were determined as per American Society for Testing and Materials (ASTM) specifications. The adhesion of the plates was evaluated by bend test (ASTM B 571-91). Thickness and hardness of the plates were determined as per ASTM B 499-88 and E 364-99, respectively. The porosity of the coatings was characterized using ferroxyl reagent test [17]. A solution of potassium ferricyanide, sodium chloride, and agar-agar in hot water was used as the ferroxyl reagent. The morphology of the plates was analyzed by using SEM after etching in 2% HCl for 2 min. The elemental composition of the coatings was determined by energy-dispersive X-ray analysis.

Electrochemical characterization

The activity of the plates towards HER was assessed by studying the galvanostatic cathodic polarization behavior of the plates in 32% NaOH electrolyte. The electrocatalytic activity of the plates with regard to HER in 32% NaOH was evaluated from the Tafel plot of the overpotential versus varying cathodic current density. The impedance analysis of the plates was also carried out at different hydrogen overpotential values to study the electrocatalytic activity of the plates at different overpotentials. To evaluate the extent of adsorption of hydrogen on the plate, the plates were initially cathodically polarized at −1.25 V in such a way that hydrogen was adsorbed on the plates. The potential was then reversed to −0.65 V. The current at −0.65 V, under the potentiostatic conditions, was then

Fig. 1 The TEM micrographs of the IrO$_2$–TiO$_2$ mixed oxide prepared by **a** TD method and **b** TO method
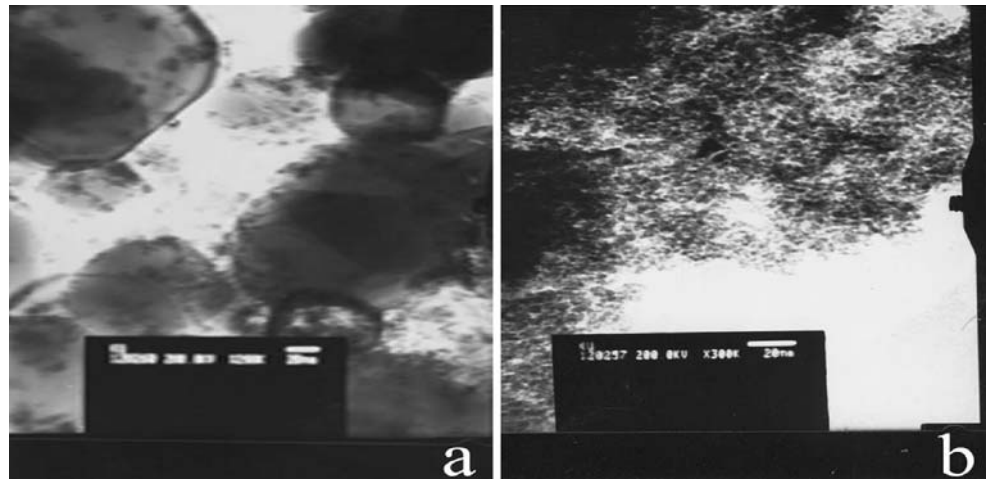
monitored as a function of time. At this potential value, it was assumed that hydrogen was oxidized.

One of the major problems of Ni–P plates is their low catalytic stability during HER in alkaline electrolyte. The stability of the catalytic activity depends on the overall stability of the plates. A change in the polarization resistance is representative of the corrosion resistance at open circuit condition. The Rp value of the plates at the open circuit condition was determined by using impedance analysis to study the corrosion behavior of the plates in 32% NaOH electrolyte. An impedance spectrometer of Autolab PGSTAT 30 with FRA2 software of FRA version 4.9 was used. The analysis was carried out in the frequency range from 1 MHz to 10 Hz. The polarization studies were carried out by using a potentiostat, electrochemical analyzer system, BAS-50 W. A platinum grid was the counter electrode and Hg/HgO/1N OH$^-$ electrode with Luggin capillary was used as the reference electrode.

Results and discussion

Characterization of the mixed oxide particles

The XRD analysis of the mixed oxides prepared by TO and TD methods was carried out, and the results confirmed the complete conversion of IrCl$_3$ into IrO$_2$. The transmission electron micrographs of the mixed oxides (Fig. 1) showed that the particle size of IrO$_2$ prepared by TO method was in very small nano scale size of ~5 nm. The IrO$_2$ particles prepared by TD method had the average particle size of ~90 nm.

Physico-chemical characterization of the plates

The TiO$_2$-supported IrO$_2$ mixed oxides prepared by following both TD and TO methods were co-deposited into electroless Ni–P plates. During the electroless Ni

Table 1 Physico-chemical characteristics of the Ni–P electroless plates with and without TiO$_2$-supported IrO$_2$ reinforcement

| Mixed oxide composition (%)		IrO$_2$ preparation method	Coating composition (%)			Thickness (μm)	Hardness (HVN)	Wear resistance
IrO$_2$	TiO$_2$		P	Ti	Ir			
0	0	–	10.4	0	0	8–10	430	Fair
0	100	–	10.2	2.6	0	9–11	550	Very good
2	98	TD	10.3	2.6	0.06	8–10	545	Good
5	95	TD	10.4	2.5	0.17	9–10	555	Good
10	90	TD	10.1	2.5	0.28	9–10	546	Good
25	75	TD	10.3	2.3	0.59	9–10	543	Good
35	65	TD	9.6	2.1	0.97	8–10	534	Good
2	98	TO	10.6	2.5	0.07	7–9	553	Good
5	95	TO	9.5	2.5	0.15	8–10	534	Good
10	90	TO	10.3	2.4	0.29	7–10	545	Good
25	75	TO	9.4	2.4	0.62	8–10	567	Good
35	65	TO	10.4	1.9	0.99	9–11	554	Good
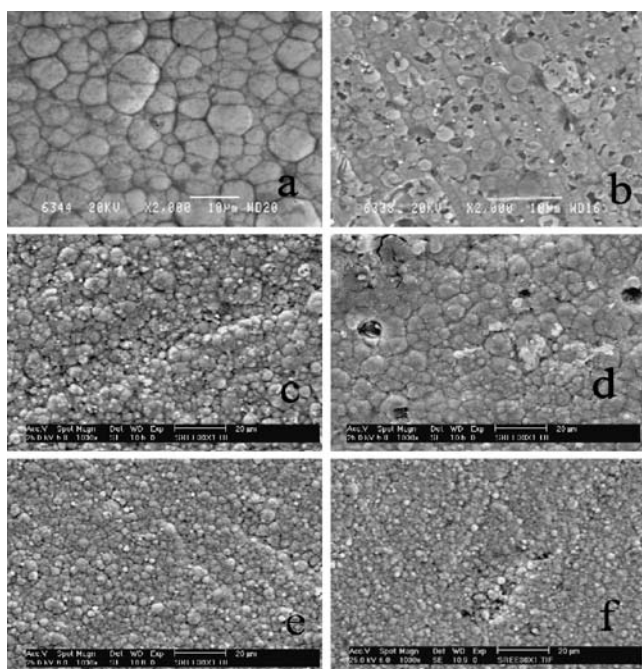
Fig. 2 The surface morphology of non-reinforced and composite-reinforced Ni–P plates before and after HER. **a** Non-reinforced, before HER. **b** Non-reinforced, after HER. **c** Reinforced with mixed oxide prepared by TD method, before HER. **d** Reinforced with mixed oxide prepared by TD method, after HER. **e** Reinforced with mixed oxide prepared by TO method, before HER. **f** Reinforced with mixed oxide prepared by TO method, after HER

plating process, the reducing agent is oxidized, and the Ni^{2+} ions are reduced on the activated substrate. The Ni, once deposited, acts as a catalyst for further deposition of Ni. In the case of electroless Ni-based composite plating, during the redox reaction between Ni^{2+} ions and the reducing agent, the composite particles, dispersed by stirring the bath, are physically entrapped in the growing layer of the Ni–P plating. The initially incorporated composite particles generally acts as active nucleation sites for further plating process. Deposition is nucleated at several catalytic surface sites, and the deposit grows both laterally and vertically to cover the entire surface entrapping the composite particles in it [18, 19].

The physical properties of the Ni–P plates with and without IrO_2–TiO_2 mixed oxide reinforcement are compared in Table 1. All the plates were found to be porous as evidenced during the ferroxyl reagent test. Typical Prussian blue coloration was observed in all the plates during the ferroxyl reagent test. Adherence and wear resistance were good for all the plates. The hardness value of the TiO_2-reinforced Ni–P plates was found to be considerably higher than that of the pure Ni–P plates. This is a general observation when hard composites, such as TiO_2, were used for reinforcing Ni–P plates [16, 20]. The hardness values of the mixed oxide reinforced plates were also same as that of the TiO_2-reinforced Ni–P plates. Hence, it was

inferred that TiO_2, which is the major component in the mixed oxide, was mostly influencing the hardness of the mixed oxide reinforced plates.

The phosphorous content of all the plates, which would have influenced the physical properties of the plates, was found to be almost same. Thus, variation in the phosphorous content was not the reason for the observed physical property changes. Hence, the physical properties of the plates were influenced mainly by titanium dioxide.

Morphological change of the plates due to TiO_2-supported IrO_2 mixed oxide reinforcement

The selection of an electrode for HER depends on the actual intrinsic electrocatalytic activity of the electrode, the
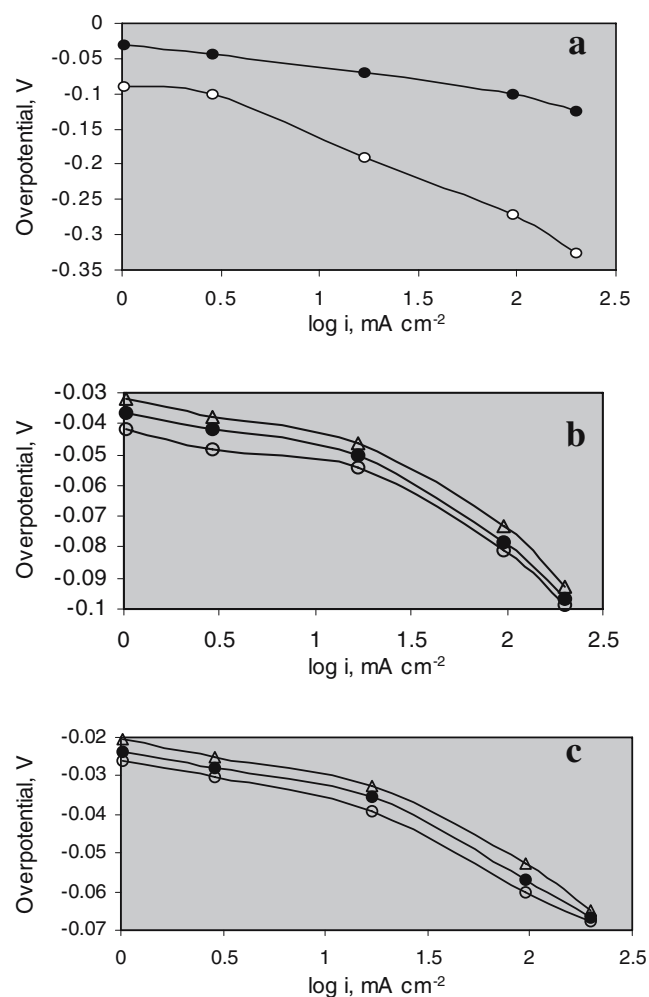

Fig. 3 Comparison of the polarization behavior of Ni–P plates, **a** with (*filled circle*) and without (*open circle*) TiO_2 reinforcement. **b** Reinforced with IrO_2–TiO_2 mixed oxide, prepared by TD method, having different percentages of IrO_2: *open circle*, 10% IrO_2; *filled circle*, 25% IrO_2; *open triangle*, 35% IrO_2. **c** Reinforced with IrO_2–TiO_2 mixed oxide, prepared by TO method, having different percentages of IrO_2: *open circle*, 10% IrO_2; *filled circle*, 25% IrO_2; *open triangle*, 35% IrO_2

Table 2 The major Tafel parameters observed for the Ni–P electroless plates with and without IrO$_2$–TiO$_2$ reinforcement

Mixed oxide composition (%)		IrO$_2$ preparation method	Overpotential (mV) at i=200 mA cm^{-2}	Tafel slope (mV dec^{-1})	Exchange current density (A cm^{-2})
IrO$_2$	TiO$_2$				
0	0	–	325	105	3.63×10^{-6}
0	100	–	125	40	8.72×10^{-6}
25	75	TD	96	33	1.56×10^{-5}
35	65	TD	95	32	1.52×10^{-5}
25	75	TO	69	30	9.65×10^{-5}
35	65	TO	68	29	9.73×10^{-5}

large surface area per unit volume ratio, and catalyst stability. The surface area per unit volume depends significantly on the surface morphology of the electrode. The surface morphology of the electrodes prepared in the present study is compared in Fig. 2. The pure Ni–P electrode was found to have well-refined grains with definite boundaries. The electrodes reinforced with TiO$_2$-supported IrO$_2$ mixed oxide prepared by TD method were found to have corrugated surface structure with uniform composite distribution. The Ni–P plates reinforced with TiO$_2$-supported IrO$_2$ mixed oxide, containing nano IrO$_2$ (prepared by TO method), was found to have uniform nodule like distribution of composite all over the surface. Thus, the surface morphology of the composite reinforced plates was more rough and corrugated compared to that of the pure Ni–P plates. Electrochemical reactions such as HER are essentially surface reactions; hence, high roughness of the composite reinforced plates would result in high reaction rate.

Evaluation of the electrocatalytic activity of the plates towards HER

The HER was carried out with all the plates in 32% NaOH solution. The Tafel plots of the electrodes are compared in Fig. 3. The pure Ni–P plate had overpotential of 325 mV at a current density of 200 mA cm^{-2}. The exchange current density observed for the pure Ni–P plate was 3.6×10^{-6} A cm^{-2}. The reinforcement with TiO$_2$ lowered the overpotential value to 125 mV and increased the exchange current density to 8.7×10^{-6} A cm^{-2}. This is due to the enhancement of the electrocatalytic activity of the plates by TiO$_2$ via existing in redox systems, TiO$_2 \leftrightarrow$ Ti$_2$O$_3 \leftrightarrow$ 2 TiOOH [21]. All the plates reinforced with IrO$_2$–TiO$_2$ mixed oxide (prepared by TD method) containing >10% IrO$_2$ exhibited an optimum lower overpotential of ~95 mV at a current density of 200 mA cm^{-2}. The exchange current density observed for these plates was ~1.5×10^{-5} A cm^{-2}. No further pronounced decrease in overpotential and increase in exchange current density was observed by increasing the amount of IrO$_2$ in the mixed oxide above
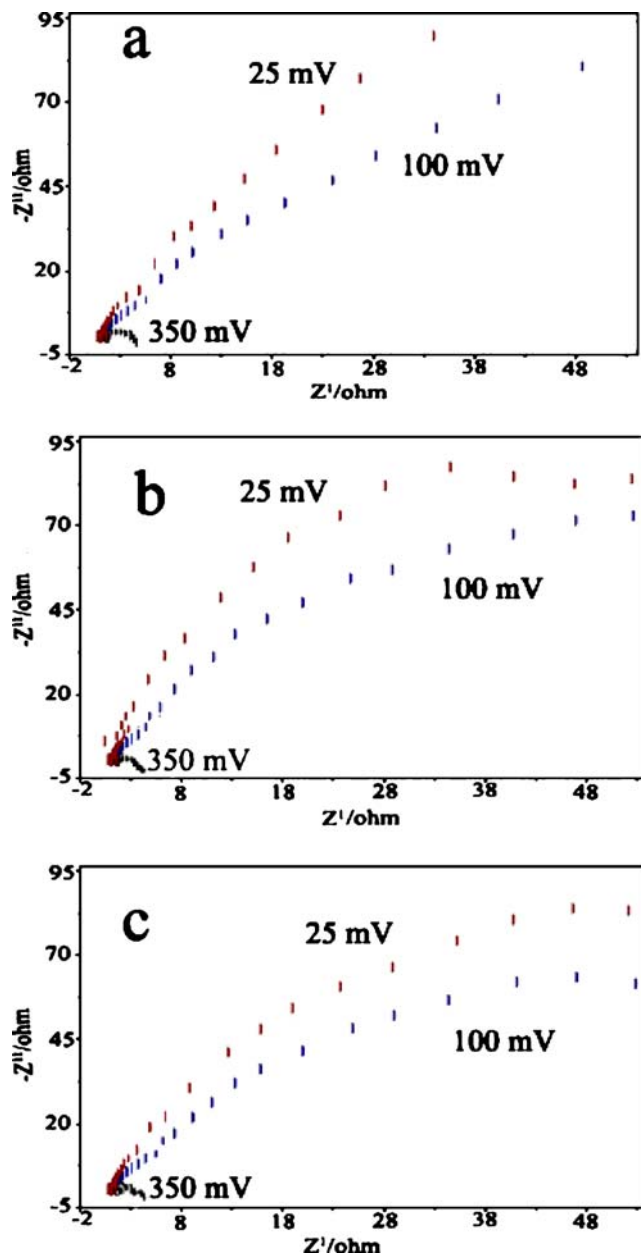

Fig. 4 The impedance behavior of the Ni–P plates with and without IrO$_2$–TiO$_2$ reinforcement at different overpotentials. **a** Pure Ni–P plate, **b** Ni–P plate reinforced with IrO$_2$–TiO$_2$ mixed oxide prepared by TD method, and **c** Ni–P plate reinforced with IrO$_2$–TiO$_2$ mixed oxide prepared by TO method

10%. All the plates reinforced with IrO_2–TiO_2 mixed oxide (prepared by TO method) containing >10% IrO_2 exhibited an optimum lower overpotential of ~70 mV at a current density of 200 mA cm^{-2}. The exchange current density observed for these plates was ~9.6×10^{-5} A cm^{-2}. In this case also, no further pronounced decrease in overpotential and increase in exchange current density was observed by increasing the amount of IrO_2 in the mixed oxide above 10%.

The Tafel slope of the pure Ni–P plate was found to be 105 mV dec^{-1}. The TiO_2-reinforced plates exhibited the Tafel slope of 40 mV dec^{-1}. Irrespective of the preparation method of the mixed oxide, the Tafel slope of TiO_2-supported IrO_2 mixed oxide-reinforced plates was ~33 mV dec^{-1}. These observations indicated the possible change of the hydrogen evolution rate-determining step from Volmer (in the case of Ni–P plate) to Heyrovsky and Tafel step (in the case of TiO_2 and TiO_2-supported IrO_2-reinforced plates). The Tafel parameters of the plates studied in the present work are compared in Table 2.

Characterization of the electrocatalytic activity by EIS

The electrochemical impedance spectroscopy (EIS) analysis of the plates was carried out at various overpotential values. The total electrical equivalent model of HER on metal electrode consists of a solution resistance R_s in series with a parallel connection of the double layer capacitance C_{dl} and a faradaic impedance Z_f. For the solid electrodes, the double layer capacitance is substituted by a constant phase element (CPE). The impedance of CPE is given by

$$Z_{CPE} = \frac{1}{T(j\omega)^{\varphi}}$$

where, φ is related to the constant phase angle $a = 90°(1-\varphi)$ and T is a capacity parameter. T is related to the solution resistance R_s and the charge transfer resistance R_{ct} as

$$T = C_{dl}^{\varphi}\left(R_s^{-1} + R_{ct}^{-1}\right)^{1-\varphi}$$

The typical models for the HER on solid, rough, or porous electrodes are (1) the CPE model [22], (2) the porous electrode model [23], and (3) a two CPE model

[22]. In CPE model, C_{dl} is substituted by CPE as described before. The porous ac impedance model predicts formation of a straight line at 45° at high frequencies and a semicircle at lower frequencies in complex plane plots. The two CPE model explaining the impedance behavior of the electrode containing pear-shaped pores is represented as the R_s in series with two CPE-R elements. This model predicts two semicircles where the high frequency semicircle is related to the surface porosity, and the low frequency semicircle is related to the charge-transfer process.

The typical Nyquist plots obtained for the Ni–P plates with and without the TiO_2-supported IrO_2 mixed oxide reinforcement are compared in Fig. 4. The major impedance parameters are given in Table 3. A single semicircle was obtained at all the overpotential values. The distortion of the semicircles observed in the present study was due to the porous nature of the plates. Complex non-linear least-square fitting program was used for the evaluation of the impedance parameters. It was observed that, for all the plates, the CPE model that includes uncompensated solution resistance R_s in series with a parallel connection of a charge transfer resistance R_{ct} and a CPE gave good approximation.

The R_{ct} values were found to be lower for the TiO_2-supported IrO_2 mixed oxide-reinforced plates at all the overpotential values. Moreover, the extent of decrease in the R_{ct} values with increase in overpotential was higher in the case of the reinforced plates. Among all the composite reinforced plates, the plate reinforced with the TiO_2-supported IrO_2 mixed oxide prepared by the TO method exhibited lower R_{ct} values, at all the overpotentials, than that of the plates reinforced with mixed oxide prepared by the TD method. This observation revealed that the TiO_2-supported IrO_2 mixed oxide reinforcement enhanced the activity of the plate towards HER, and the particle size of the electrocatalytic metal oxide, IrO_2, has high effect on inducing activation of the plates.

The C_{dl} values calculated from CPE values by using the Brug equation [24] are compared in Table 3. C_{dl} values were found to be higher for the TiO_2-supported IrO_2 mixed oxide-reinforced plates. The highest C_{dl} values were observed for the plates reinforced with mixed oxide

Table 3 The electrochemical impedance parameters of the Ni–P plates with and without composite reinforcement observed at different overpotential values

Composite in the coating	η (mV)	R_{ct} (Ω)	φ	C_{dl} (F)	R_f
Without composite	25	8.5×10^3	0.752	1.09×10^{-4}	5.45
	100	7.9×10^2	0.634	5.53×10^{-4}	27.65
	350	4.8×10^0	0.765	7.25×10^{-4}	36.25
IrO_2–TiO_2 made by TD	25	9.9×10^2	0.731	1.21×10^{-3}	60.50
	100	5.4×10^2	0.629	4.14×10^{-3}	207.0
	350	4.6×10^0	0.724	4.15×10^{-3}	207.5
IrO_2–TiO_2 made by TO	25	8.6×10^2	0.733	1.68×10^{-3}	84.00
	100	4.3×10^2	0.623	4.56×10^{-3}	228.0
	350	3.7×10^0	0.613	4.43×10^{-3}	221.5

containing nano IrO_2 prepared by using TO method. The lower R_{ct} and higher C_{dl} values observed in the case of TiO_2-supported IrO_2 mixed oxide-reinforced plates at different overpotentials indicate that the active surface area has been increased by reinforcement. The same argument also points out that the increase in active surface area is higher for the plates reinforced with TiO_2-supported IrO_2 mixed oxide containing nano IrO_2 prepared by TO method.

The parameter φ is related to the surface roughness of the electrodes. The deviation of φ from the value of 1 can reveal the change in surface roughness. From the values of φ given in Table 3, it is clear that at all the overpotential values, larger deviations of φ from the value of 1 occurred in the TiO_2-supported IrO_2 mixed oxide-reinforced plates. This observation indicates that high change in surface roughness occurred in the case of the plates with reinforcement. The surface roughness factor R_f of the plates was calculated from the ratio of the double layer capacitance C_{dl} of the tested plates and the C_{dl} of the smooth metallic electrode, which is taken as 20 μF cm^{-2} [25]. Thus $R_f = C_{dl}/20$ μF cm^{-2}. The R_f values (Table 3) indicated that the composite reinforced plates had higher roughness values. The R_f factor was found to be highest for the plates reinforced with TiO_2-supported IrO_2 mixed oxide containing nano IrO_2 prepared by TO method. Hence, the highest active surface area and the highest surface roughness of the mixed oxide-reinforced plates, especially the plates reinforced with mixed oxide containing very small nano size catalytic metal oxide particles prepared by TO method, facilitated HER.
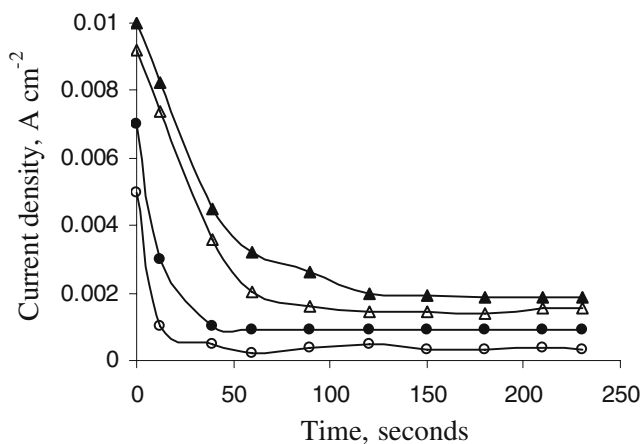
The extent of hydrogen adsorption

In another set of experiments, the electrodes were cathodically polarized at −1.25 V in such a way that hydrogen was adsorbed on the electrode. Then, the potential was reversed to −0.65 V. At this potential value, it was assumed that hydrogen was oxidized. Figure 5 shows the variation in current density with time after the potential was reversed to −0.65 V. The current density was decreased with time, and

Fig. 5 The current density variation during potentiostatic experiment at −0.65 V in 32% NaOH solution after the electrodes have been cathodically polarized at −1.25 V. *Open circle*, pure Ni–P plate; *filled circle*, TiO_2-reinforced Ni–P plate; *open triangle*, Ni–P plate reinforced with TiO_2-supported IrO_2 prepared by TD method; *filled triangle*, Ni–P plate reinforced with TiO_2-supported IrO_2 prepared by TO method
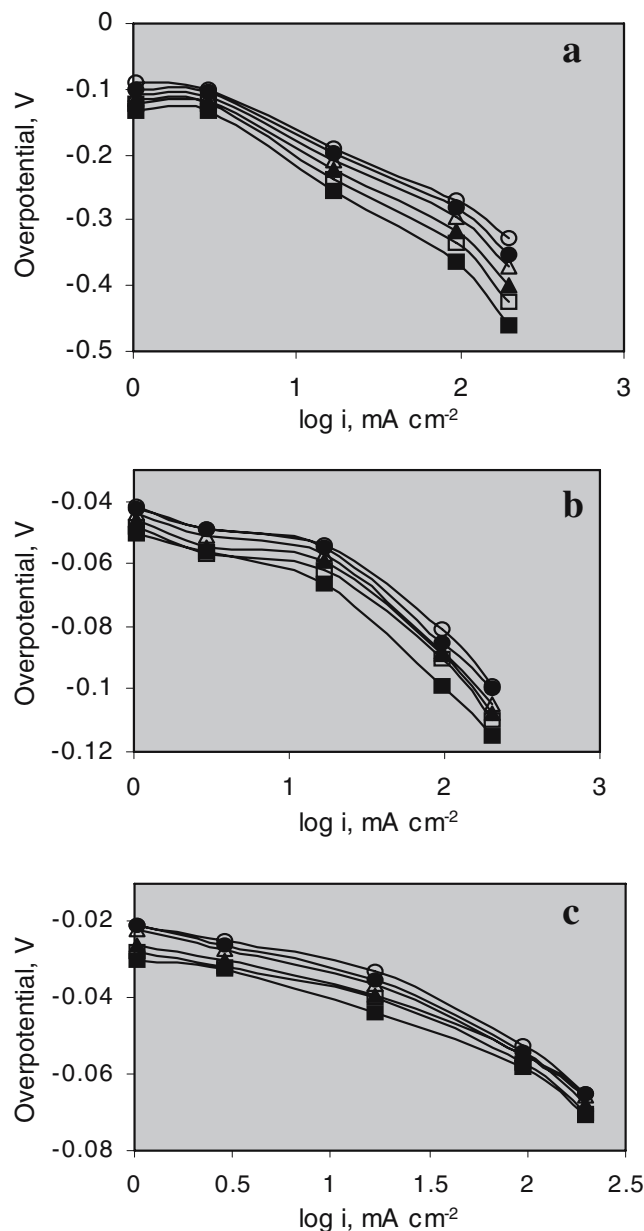

Fig. 6 The polarization behavior of the pure and composite reinforced Ni–P plates observed after different durations of HER; **a** without reinforcement, **b** reinforcement with IrO_2–TiO_2 prepared by TD method, **c** reinforcement with IrO_2–TiO_2 prepared by TO method. *Open circle*, before HER; *filled circle*, after HER for 10 h; *open triangle*, after HER for 20 h; *filled triangle*, after HER for 30 h; *open square*, after HER for 40 h; *filled square*, after HER for 50 h

a plot of the observed current density versus the inverse of the square root of the time (Cottrell plot) was found to be straight line. Hence, it was assumed that the observed current density is a diffusion current density due to the oxidation of adsorbed hydrogen on the electrode. An idea about the extent of hydrogen adsorbed on the electrode surface can be obtained from the area under the current density–time curve. It is clear from Fig. 5 that the extent of hydrogen adsorption on the plates reinforced with TiO_2-supported IrO_2 mixed oxide was higher. The extent of hydrogen adsorption on the different electrode surface, studied in the present work, showed the same trend as the observed electrocatalytic activity of the electrodes towards HER.

Stability of catalytic activity of the plates

The plates were subjected to HER for 50 h at a current density of 200 mA cm^{-2}. After each 10 h, the plates were washed with distilled water and dried. Then, the galvanostatic cathodic polarization of the plates in 32% NaOH solution was carried out. The Tafel plots obtained during the study of the electrodes are compared in Fig. 6. After each 10 h of hydrogen evolution, no considerable change in the Tafel plots in terms of Tafel slope or overpotential was observed for the mixed oxide reinforced plates. The pure Ni–P plates exhibited somewhat more increase in overpotential. However, no change in the Tafel slope was observed in the case of the pure Ni–P plates also. This analysis revealed the stability of the electrocatalytic activity of the mixed metal oxide-reinforced plates.

The change in the morphology of the plates because of hydrogen evolution for 100 h at a current density of 200 mA cm^{-2} is also shown in Fig. 1. The Ni–P plates showed blisters and plating failures at some regions. The composite reinforced plates did not exhibit considerable morphological change. This observation confirms the stability of the composite-reinforced plates during HER.

Conclusions

Nickel–phosphorous alloy electroless plates were reinforced with TiO_2-supported IrO_2 mixed oxide composite. Different size of electrocatalytic IrO_2 particles were used to reinforce the plates. The electrodes were evaluated for HER. The physical characteristics of the TiO_2-supported

IrO_2 mixed oxide-reinforced Ni–P plates were found to be better than that of the pure Ni–P plates. The composite reinforced plates had high stability in alkaline electrolyte. The electrodes exhibited high catalytic activity for HER. The activity of the electrodes was found to be highly dependent on the particle size of the IrO_2 catalytic particles. The electrodes containing IrO_2 particles of small size in nano scale exhibited very high activity. The catalytic activity of the plates was found to be stable during long-term HER.

References

1. Veziroglu TN, Barbir F (1992). Int J Hydrogen Energy 17:391
2. Trasatti S (1992) In: Wellington TC (ed) Modern chlor–alkali technology. Elsevier, Amsterdam, p 281
3. Tavares AC, Trasatti S (2000) Electrochim Acta 45:4195
4. Chiaki I, Masashi T, Shuji N, Hiroshi I, Masao M, Naoji F (1995) Electrochim Acta 40:977
5. Chiaki I, Naoji F, Masashi T (1992) Electrochim Acta 37:757
6. Chen L, Guay D, Lasia A (1996) J Electrochem Soc 143:3576
7. Chen H, Trasatti S (1993) J Electroanal Chem 357:91
8. Boots JCF, Trasatti S (1989) J Appl Electrochem 19:255
9. Losiewiez B, Budniok A, Rowinski E, Lagiewka E, Lasia A (2004) Int J Hydrogen Energy 29:145
10. Tsou Y (2001) J Electroanal Chem 498:223
11. Iwakura C, Tonaka M, Nakamatsu S, Inoue H, Matsuoka M, Furukawa N (1995) Electrochim Acta 40:977
12. Shibli SMA, Dilimon VS, Deepthi T (2006) Appl Surf Sci (In press)
13. Gierlotka D, Rovinski E, Budniok A, Lagiewka E (1997) J Appl Electrochem 27:1349
14. Crnkovic FC, Machado SAS, Avaca LA (2004) Int J Hydrogen Energy 29:249
15. Adams R, Shriner RL (1923) J Am Chem Soc 45:2171
16. Balaraju JN, Sankara Narayanan TS, Seshadri SK (2003) J Appl Electrochem 33:807
17. Koehler WA, Burford RO (1936) Trans Electr Soc 70:397
18. Sharma SB, Agarwala RC, Agarwala V, Satyanarayana KG (2005) Metall Mater Trans B 36:23
19. Cattarin S, Musiani M (2006) Electrochim Acta. DOI 10/1016/j.electacta.2006.07.035. (in press, available online at http://www.sciencedirect.com)
20. Hussain MS, Such TE (1985) Surf Technol 13:119
21. Gierlotka D, Rovinski E, Budniok A, Lagiewka E (1997) J Appl Electrochem 27:1349
22. Lasia A (2002) In: Conway BE, White RE (eds) 'Modern aspects of electrochemistry', vol 35. Plenum, New York, p 1
23. de Levie R (1967) In: Delahay P (ed) 'Adv Electrochem Electrochem Eng' vol 6. Interscience, New York, p 326
24. Brug GJ, Van Der Eeden ALG, Sluyters-Rehbach M, Sluyters JH (1984) J Electroanal Chem 176:275
25. Karimi Shervedani R, Lasia A (1997) J Electrochem Soc 144:8